Acta Cryst E
CRYSTALLOGRAPHIC COMMUNICATIONS

ISSN 2056-9890

Crystal structure, Hirshfeld surface analysis and corrosion inhibition study of 3,6-bis(pyridin-2-yl)-4-{[(3a*S*,5*S*,5a*R*,8a*R*,8b*S*)-2,2,7,7-tetramethyltetrahydro-5*H*-bis[1,3]dioxolo[4,5-*b*:4′,5′-*d*]pyran-5-yl)methoxy]methyl}pyridazine monohydrate

Mouad Filali,[a]* Hicham Elmsellem,[b] Tuncer Hökelek,[c] Abdelkrim El-Ghayoury,[d] Oleh Stetsiuk,[d] El Mestafa El Hadrami[a] and Abdessalam Ben-Tama[a]

[a]Laboratoire de Chimie Organique Appliquée, Université Sidi Mohamed Ben Abdallah, Faculté des Sciences et Techniques, Route d'Immouzzer, BP 2202, Fez, Morocco, [b]Laboratoire de Chimie Analytique Appliquée, Matériaux et Environnement (LC2AME), Faculté des Sciences, BP 717, 60000 Oujda, Morocco, [c]Department of Physics, Hacettepe University, 06800 Beytepe, Ankara, Turkey, and [d]Laboratoire MOLTECH-Anjou, UMR 6200, CNRS, UNIV Angers 2 bd Lavoisier, 49045 Angers Cedex, France. *Correspondence e-mail: mmouadfilali10@gmail.com

Received 4 June 2019
Accepted 9 July 2019

Edited by A. J. Lough, University of Toronto, Canada

Keywords: crystal structure; pyridazine; dioxolo; Hirshfeld surface; electrochemical measurements.

CCDC reference: 1939591

Supporting information: this article has supporting information at journals.iucr.org/e

In the title compound, $C_{27}H_{30}N_4O_6{\cdot}H_2O$, the two dioxolo rings are in envelope conformations, while the pyran ring is in a twisted-boat conformation. The pyradizine ring is oriented at dihedral angles of 9.23 (6) and 12.98 (9)° with respect to the pyridine rings, while the dihedral angle between the two pyridine rings is 13.45 (10)°. In the crystal, $O—H_{water}\cdots O_{pyran}$, $O—H_{water}\cdots O_{methoxymethyl}$ and $O—H_{water}\cdots N_{pyridazine}$ hydrogen bonds link the molecules into chains along [010]. In addition, weak $C—H_{dioxolo}\cdots O_{dioxolo}$ hydrogen bonds and a weak $C—H_{methoxymethyl}\cdots\pi$ interaction complete the three-dimensional structure. The Hirshfeld surface analysis of the crystal structure indicates that the most important contributions for the crystal packing are from H⋯H (55.7%), H⋯C/C⋯H (14.6%), H⋯O/O⋯H (14.5%) and H⋯N/N⋯H (9.6%) interactions. Hydrogen-bonding and van der Waals interactions are the dominant interactions in the crystal packing. Electrochemical measurements are also reported.

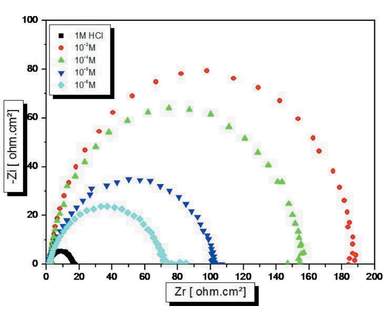

1. Chemical context

Given their importance in the pharmaceutical, chemical and industrial fields, the synthesis of 3,6-di(pyridin-2-yl)pyridazine and its derivatives has been a goal of chemists in recent years. 5-[3,6-Di(pyridin-2-yl)pyridazine-4-yl]-2′-deoxyuridine-5′-*O*-triphosphate can be used as a potential substrate for fluorescence detection and imaging of DNA (Kore *et al.*, 2015). Systems containing this moiety have also shown remarkable corrosion inhibitory (Khadiri *et al.*, 2016). Heterocyclic molecules such as 3,6-bis (2′-pyridyl)-1,2,4,5-tetrazine have been used in transition-metal chemistry (Kaim & Kohlmann, 1987). This bidentate chelate ligand is popular in coordination chemistry and complexes of a wide range of metals, including iridium and palladium (Tsukada *et al.*, 2001). We report herein the synthesis and the molecular and crystal structures of the title compound, (I), along with the Hirshfeld surface analysis and its corrosion inhibition properties.

2. Structural commentary

The title molecule contains two dioxolo, two pyridine, one pyridazine and one pyran rings (Fig. 1). The pyridazine ring is linked to the pyran ring through the methoxymethyl moiety.

The two dioxolo rings, *B* (O2/O3/C2–C4) and *C* (O4/O5/C5–C7), are in envelope conformations. Atoms O3 and O4 are at the flap positions and are displaced by 0.442 (2) and −0.397 (2) Å, respectively, from the least-squares planes of the four atoms. A puckering analysis of the pyran ring *A* (O1/C1/C2/C4–C6), gave the parameters Q_T = 0.6508 (25) Å, q_2 = 0.6451 (25) Å, q_3 = −0.0865 (26) Å, φ = 214.6 (2)° and θ = 97.64 (23)°, indicating a twisted-boat conformation. The pyradizine ring *D* (N1/N2/C14–C17) is oriented at dihedral angles of 9.23 (6) and 12.98 (9)°, respectively, to the pyridine rings *E* (N3/C18–C22) and *F* (N4/C23–C27), while the dihedral angle between the two pyridine rings is 13.45 (10)°. The methoxymethyl moiety is nearly co-planar with the pyradizine ring, as indicated by the O6—C13—C14—C15 torsion angle of −172.8 (2)°.

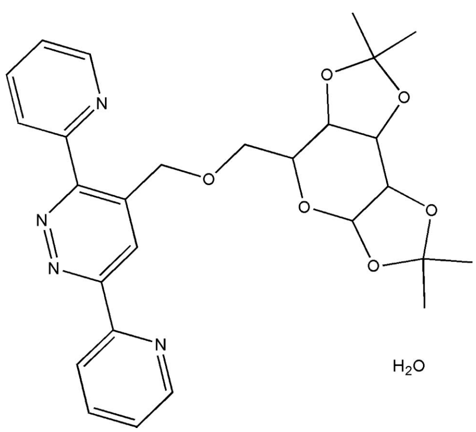

3. Supramolecular features

In the crystal, O—$H_{water}\cdots O_{pyran}$, O—$H_{water}\cdots O_{methoxymethyl}$ and O—$H_{water}\cdots N_{pyridazine}$ hydrogen bonds (Table 1 and Fig. 2) link the molecules, forming chains along [010]. The hydrogen bond involving H7*B* is bifurcated. In addition, weak C—$H_{dioxolo}\cdots O_{dioxolo}$ hydrogen bonds and a weak C—$H_{methoxymethyl}\cdots\pi$ interaction complete the three-dimensional structure.

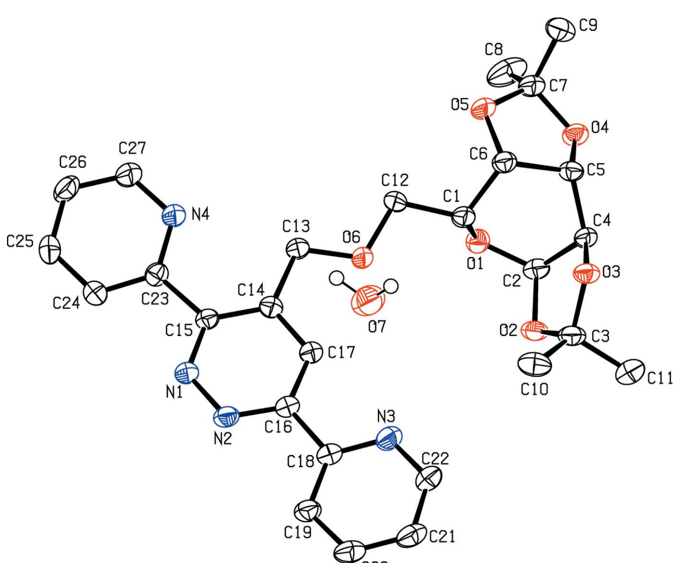

Figure 1
The molecular structure of the title compound with the atom-numbering scheme. Displacement ellipsoids are drawn at the 50% probability level. H atoms bonded to C atoms are not shown.

Table 1
Hydrogen-bond geometry (Å, °).

Cg is the centroid of the N3/C18–C22 ring.

D—H···*A*	*D*—H	H···*A*	*D*···*A*	*D*—H···*A*
O7—H7*A*···N2^{i}	0.84 (2)	2.18 (3)	3.019 (4)	172 (6)
O7—H7*B*···O1	0.86 (2)	2.30 (3)	3.112 (4)	157 (6)
O7—H7*B*···O6	0.86 (2)	2.57 (5)	3.176 (5)	129 (5)
C2—H2···O3^{ii}	0.98	2.51	3.444 (4)	160
C12—H12*A*···*Cg*^{iv}	0.97	3.07	3.761 (3)	130

Symmetry codes: (i) $-x, y-\frac{1}{2}, -z+\frac{1}{2}$; (ii) $x-\frac{1}{2}, -y+\frac{1}{2}, -z+1$; (iv) $-x+1, y-\frac{1}{2}, -z+\frac{1}{2}$.

4. Hirshfeld surface analysis

In order to visualize the intermolecular interactions in the crystal of the title compound, a Hirshfeld surface (HS) analysis (Hirshfeld, 1977; Spackman & Jayatilaka, 2009) was carried out by using *CrystalExplorer17.5* (Turner *et al.*, 2017). In the HS plotted over d_{norm} (Fig. 3), white indicates contacts with distances equal to the sum of van der Waals radii, while red and blue indicate distances shorter (in close contact) or longer (distinct contact) than the van der Waals radii, respectively (Venkatesan *et al.*, 2016). The bright-red spots appearing near O1, O6, N2 and hydrogen atoms H2, H7*A*, H7*B* indicate their roles as the respective donors and/or acceptors. The shape-index of the HS is a tool to visualize the π–π stacking by the presence of adjacent red and blue triangles; if these are absent, then there are no π–π interactions. Fig. 4 clearly suggest that there are no π–π interactions in (I). The overall two-dimensional fingerprint plot, Fig. 5*a*, and those delineated into H···H, H···C/C···H, H···O/O···H, H···N/N ···H, C···C and C···N/N···C contacts (McKinnon *et al.*, 2007) are illustrated in Fig. 5*b*–*g*, respectively, together with their relative contributions to the Hirshfeld surface. Selected contacts are listed in Table 2.

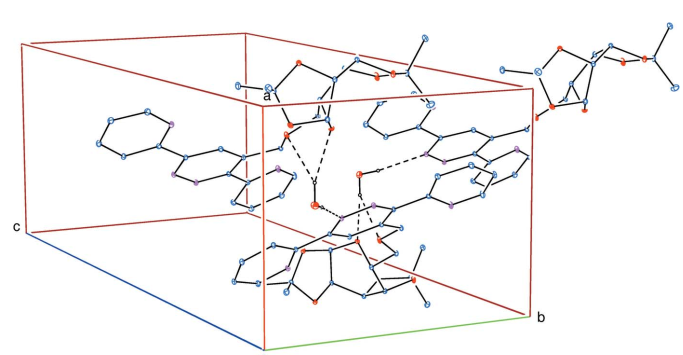

Figure 2
A partial packing diagram showing the O—$H_{water}\cdots O_{pyran}$, O—$H_{water}\cdots O_{methoxymethyl}$ and O—$H_{water}\cdots N_{pyridazine}$ hydrogen bonds (Table 1) as dashed lines.

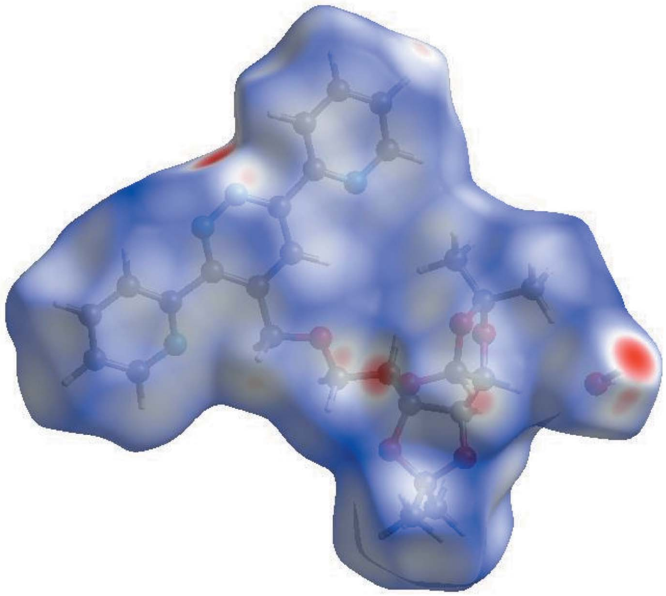

Figure 3
View of the three-dimensional Hirshfeld surface of the title compound plotted over d_{norm} in the range −0.4555 to 1.4860 a.u.

The most important interaction is H⋯H, contributing 55.7% to the overall crystal packing, which is reflected in Fig. 5*b* as widely scattered points of high density due to the large hydrogen content of the molecule with the tip at $d_e = d_i$ ~1.00 Å. In the presence of a weak C—H⋯π interaction, the wings in the fingerprint plot delineated into H⋯C/C⋯H contacts (14.6% contribution to the HS) have a symmetrical distribution of points, Fig. 5*c*, with the thin and thick edges at $d_e + d_i$ = 2.85 and 2.78 Å. The pair of characteristic wings in the fingerprint plot delineated into H⋯O/O⋯H contacts (14.5%, Fig. 5*d*) arises from the O—H⋯O and C—H⋯O hydrogen bonds (Table 1) as well as from the H⋯O/O⋯H contacts (Table 2) and has a pair of spikes with the tips at $d_e + d_i$ = 2.18 Å. The pair of characteristic wings in the fingerprint plot delineated into H⋯N/N⋯H contacts (Fig. 5*e*, 9.6%) arises from the O—H⋯N hydrogen bonds (Table 1) as well as from the H⋯N/N⋯H contacts has a pair of spikes with the tips at

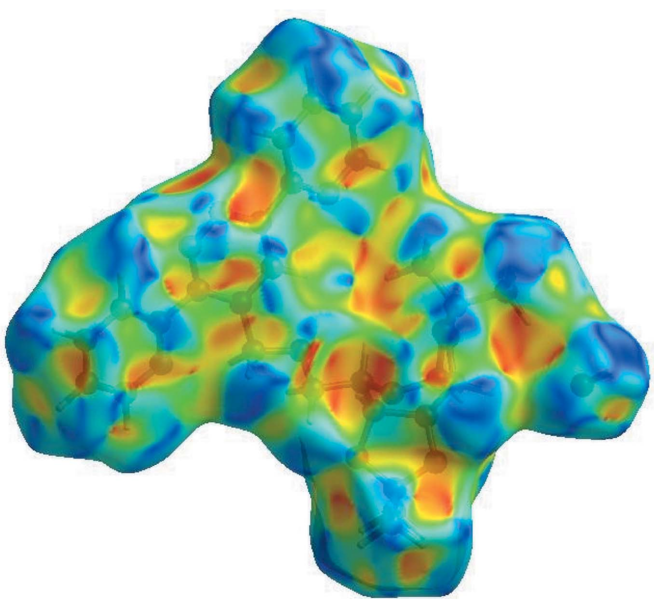

Figure 4
Hirshfeld surface of the title compound plotted over shape-index.

Table 2
Selected interatomic distances (Å).

O1⋯O3	3.153 (2)	C2⋯C4^{ii}	3.538 (4)
O1⋯O4	3.115 (3)	C2⋯H4^{ii}	2.96
O1⋯O5	2.999 (3)	C3⋯H1	2.88
O1⋯O6	2.920 (3)	C4⋯H11*A*	2.84
O3⋯O1	3.153 (2)	C4⋯H2^{iii}	2.83
O3⋯C1	3.002 (3)	C4⋯H1	2.76
O7⋯O1	3.112 (3)	C5⋯H9*A*	2.85
O7⋯O6	3.176 (3)	C10⋯H1	2.93
O7⋯N2^{i}	3.020 (3)	H1⋯H10*C*	2.24
O2⋯H1	2.70	H2⋯H4^{ii}	2.44
O2⋯H4^{ii}	2.90	H4⋯H11*A*	2.47
O3⋯H1	2.54	H5⋯H9*A*	2.56
O3⋯H2^{iii}	2.51	H7*A*⋯H19^{i}	2.20
O5⋯H12*B*	2.70	H7*A*⋯N1^{i}	2.84 (3)
O5⋯H12*A*	2.77	H7*A*⋯N2^{i}	2.19 (4)
O6⋯H17	2.23	H7*B*⋯O1	2.30 (2)
O7⋯H19^{i}	2.64	H7*B*⋯O6	2.56 (4)
N4⋯C13	2.776 (3)	H8*A*⋯H9*C*	2.55
N1⋯H24	2.44	H8*B*⋯H9*B*	2.50
N2⋯H19	2.56	H8*C*⋯H11*C*^{ii}	2.48
N3⋯H17	2.46	H10*A*⋯H11*C*	2.53
N4⋯H13*A*	2.56	H10*B*⋯H11*B*	2.57
N4⋯H13*B*	2.54	H12*A*⋯H13*B*	2.26
C1⋯C3	3.485 (3)		

Symmetry codes: (i) $-x, y-\frac{1}{2}, -z+\frac{1}{2}$; (ii) $x-\frac{1}{2}, -y+\frac{1}{2}, -z+1$; (iii) $x+\frac{1}{2}, -y+\frac{1}{2}, -z+1$.

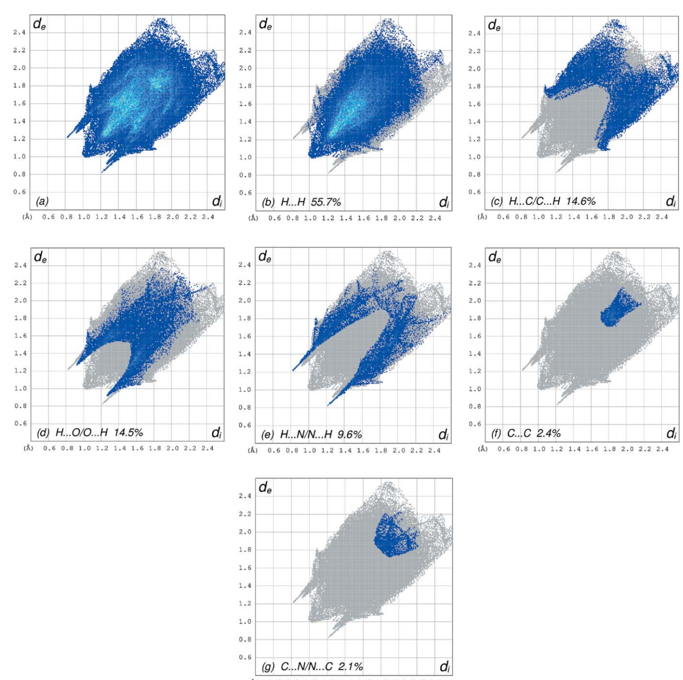

Figure 5
The full two-dimensional fingerprint plots for the title compound, showing (*a*) all interactions, and delineated into (*b*) H⋯H, (*c*) H⋯C/C⋯H, (*d*) H⋯O/O⋯H, (*e*) H⋯N/N⋯H, (*f*) C⋯C and (*g*) C⋯N/N⋯C interactions. The d_i and d_e values are the closest internal and external distances (in Å) from given points on the Hirshfeld surface.

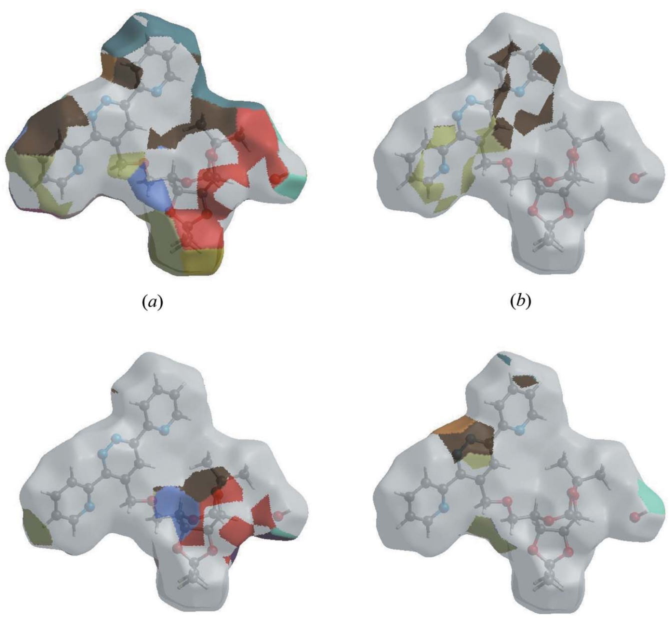

Figure 6
Hirshfeld surface representations with the function d_{norm} plotted onto the surface for (*a*) H$\cdots$H, (*b*) H$\cdots$C/C$\cdots$H, (*c*) H$\cdots$O/O$\cdots$H and (*d*) H$\cdots$N/N$\cdots$H interactions.

$d_e + d_i$ = 2.04 Å. Finally, the C$\cdots$C contacts (Fig. 5*g*, 2.4%) have a wide spike with the tip at $d_e = d_i$ = 1.75 Å.

The Hirshfeld surface representations with the function d_{norm} plotted onto the surface are shown for the H$\cdots$H, H$\cdots$C/C$\cdots$H, H$\cdots$O/O$\cdots$H and H$\cdots$N/N$\cdots$H interactions in Fig. 6*a*–*d*, respectively.

The Hirshfeld surface analysis confirms the importance of H-atom contacts in establishing the packing. The large number of H$\cdots$H, H$\cdots$C/C$\cdots$H, H$\cdots$O/O$\cdots$H and H$\cdots$N/N$\cdots$H interactions suggest that van der Waals interactions and hydrogen bonding play the major roles in the crystal packing (Hathwar *et al.*, 2015).

5. Electrochemical measurements

The effect of the title compound as an inhibitor of the corrosion of mild steel (MS) were studied using electrochemical impedance spectroscopy in the concentration range of 10^{-6} to 10^{-3} *M* at 308 K. The electrochemical experiment consisted of a 3 electrode electrolytic cell consisting of platinum foil as counter-electrode, saturated calomel as reference electrode and MS as working electrode with an exposed area of 1 cm^2. The MS specimen was immersed in a test solution for 0.5 h until a steady-state potential was achieved using a PGZ100 potentiostat (Bouayad *et al.*, 2018). Electrochemical impedance spectroscopy (EIS) measurements were performed over a frequency range of 0.1×10^{-3} KHz to 10 mHz and an amplitude of 10 mV with 10 points per decade. The percentage inhibition efficiency is calculated from R_t values as (Sikine *et al.*, 2016) $E\,(\%) = [1 - R_{t(HCl)}/R_{t(inh)}] \times 100$, where $R_{t(inh)}$ and $R_{t(HCl)}$ are the charge-transfer resistances for MS immersed in HCl, with the title compound and without inhibitor. Nyquist representations of mild steel in 1 *M* HCl in the absence and presence of the inhibitor system are shown in Fig. 7.

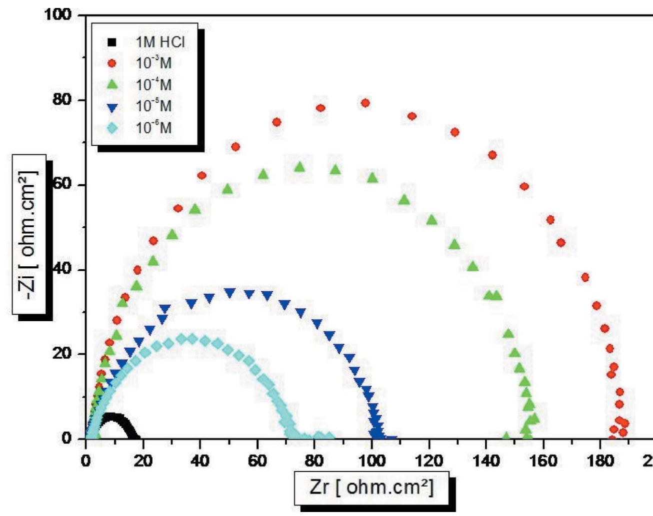

Figure 7
Nyquist plots of mild steel in 1*M* HCl in presence of different concentrations of 3,6-bis(pyridin-2-yl)-4-{[(3a*S*,5*S*,5a*R*,8a*R*,8b*S*)-2,2,7,7-tetramethyltetrahydro-5*H*-bis[1,3]dioxolo[4,5-*b*:4′,5′-*d*]pyran-5-yl)methoxy]methyl}pyridazine monohydrate.

The impedance method provides information about the kinetics of the electrode processes and the surface properties of the investigated systems. The technique is based on the measurement of the impedance of the double layer at the MS/solution interface, and represents the Nyquist plots of mild steel (MS) specimens in 1 *M* HCl without and with various concentrations of the inhibitor. The impedance diagrams obtained have an almost semicircular appearance. This indicates that the corrosion of mild steel in aqueous solution is mainly controlled by a charge-transfer process. The impedance parameters are given in Fig. 8. It is observed from the

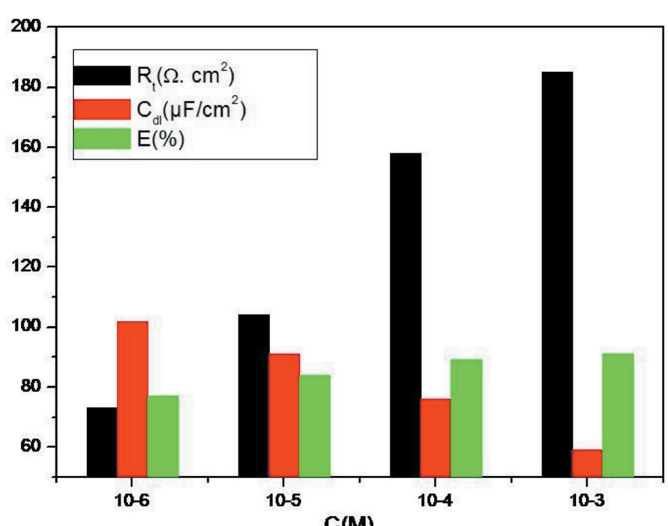

Figure 8
EIS parameters for the corrosion of mild steel in 1*M* HCl with and without inhibitor 3,6-bis(pyridin-2-yl)-4-{[(3a*S*,5*S*,5a*R*,8a*R*,8b*S*)-2,2,7,7-tetramethyltetrahydro-5*H*-bis[1,3]dioxolo[4,5-*b*:4′,5′-*d*]pyran-5-yl)methoxy]methyl}pyridazine monohydrate at 308 K.

Table 3
Experimental details.

Crystal data	
Chemical formula	$C_{27}H_{30}N_4O_6{\cdot}H_2O$
M_r	524.56
Crystal system, space group	Orthorhombic, $P2_12_12_1$
Temperature (K)	150
a, b, c (Å)	8.8417 (3), 11.3252 (3), 25.7003 (8)
V (Å^3)	2573.47 (14)
Z	4
Radiation type	Cu $K\alpha$
μ (mm^{-1})	0.82
Crystal size (mm)	0.47 × 0.15 × 0.10
Data collection	
Diffractometer	Rigaku Oxford Diffraction SuperNova, single source at offset, AtlasS2
Absorption correction	Multi-scan (*CrysAlis PRO* (Rigaku OD, 2015)
T_{min}, T_{max}	0.656, 1.000
No. of measured, independent and observed [$I > 2\sigma(I)$] reflections	6128, 4277, 3853
R_{int}	0.037
$(\sin \theta/\lambda)_{max}$ (Å^{-1})	0.618
Refinement	
$R[F^2 > 2\sigma(F^2)]$, $wR(F^2)$, S	0.048, 0.121, 1.10
No. of reflections	4277
No. of parameters	353
No. of restraints	2
H-atom treatment	H atoms treated by a mixture of independent and constrained refinement
$\Delta\rho_{max}$, $\Delta\rho_{min}$ (e Å^{-3})	0.27, −0.36
Absolute structure	Flack x determined using 1226 quotients $[(I^+)-(I^-)]/[(I^+)+(I^-)]$ (Parsons et al., 2013)
Absolute structure parameter	−0.01 (16)

Computer programs: *CrysAlis PRO* (Rigaku OD, 2015), *SHELXS97* (Sheldrick, 2008), *SHELXL2018* (Sheldrick, 2015), *ORTEP-3* for Windows and *WinGX* (Farrugia, 2012) and *PLATON* (Spek, 2015).

plots that the impedance response of mild steel was significantly changed after addition of the inhibitor. R_{ct} is increased to a maximum value of 185 Ω cm^2 for the inhibitor, showing a maximum inhibition efficiency of 91% at 10^{-3} *M*. The decrease in C_{dl} from the HCl acid value of 200 µF cm^{-2}, may be due to the increase in the thickness of the electrical double layer or to a decrease in the local dielectric constant (Elmsellem *et al.*, 2014). This is caused by the gradual displacement of water molecules by the adsorption of organic molecules on the mild steel surface (Hjouji *et al.*, 2016). Apart from the experimental impedance (EIS) results, the following conclusion is drawn: the alternating impedance spectrum reveals that the double-layer capacitances decrease with respect to the blank solution when the title compound is added. This fact confirms the adsorption of inhibitor molecules on the surface of the MS.

6. Database survey

Silver(I) complexes coordinated by 3,6-di(pyridin-2-yl)pyridazine ligands have been reported (Constable *et al.*, 2008). Three other metal complexes including 3,6-di(pyridin-2-yl)pyridazine have also been reported, *viz*. aquabis[3,6-bis(pyridin-2-yl)pyridazine-κ_2N^1,N^6]copper(II) bis(trifluoromethanesulfonate) (Showrilu *et al.*, 2017), tetrakis[μ-3,6-di(pyridin-2-yl)pyridazine]bis(μ-hydroxo)bis(μ-aqua)tetranickel(II) hexakis(nitrate) tetradecahydrate (Marino *et al.*, 2019) and *catena*-[[μ^2-3,6-di(pyridin-2-yl)pyridazine]bis(μ^2-azido)diazaidodicopper monohydrate] (Mastropietro *et al.*, 2013).

7. Synthesis and crystallization

6-*O*-Propargyl-1,2:3,4-di-*O*-isopropylidene-α-D-galactopyranoside (4 mmol) was added to a solution of 3,6-bis(2-pyridyl)-1,2,4,5-tetrazine (4 mmol) in toluene (20 ml). Stirring was continued at room temperature for 4 h. The solvent was removed under reduced pressure. The residue was separated by chromatography on a column of silica gel with ethyl acetate/hexane (1:2) as eluent. Colourless crystals were isolated on evaporation of the solvent (yield: 82%).

8. Refinement

Crystal data, data collection and structure refinement details are summarized in Table 3. Water hydrogen atoms were located in a difference-Fourier map and refined with the distance constraint O—H = 0.80 (2) Å. Other H atoms were positioned geometrically with C—H = 0.93, 0.98, 0.97 and 0.96 Å, for aromatic, methine, methylene and methyl H atoms, respectively, and constrained to ride on their parent atoms, with U_{iso}(H) = 1.5U_{eq}(C-methyl) or 1.2U_{eq}(C) for all other H atoms.

Funding information

TH is grateful to Hacettepe University Scientific Research Project Unit (grant No. 013 D04 602 004).

References

Bouayad, K., Kandri Rodi, Y., Elmsellem, H., El Ghadraoui, E. H., Ouzidan, Y., Abdel-Rahman, I., Kusuma, H. S., Warad, I., Mague, J. T., Essassi, E. M., Hammouti, B. & Chetouani, A. (2018). *Mor. J. Chem.* **6**, 22–34.
Constable, E. C., Housecroft, C. E., Neuburger, M., Reymann, S. & Schaffner, S. (2008). *Aust. J. Chem.* **61**, 847–853.
Elmsellem, H., Nacer, H., Halaimia, F., Aouniti, A., Lakehal, I., Chetouani, A., Al-Deyab, S. S., Warad, I., Touzani, R. & Hammouti, B. (2014). *Int. J. Electrochem. Sci.* **9**, 5328–5351.
Farrugia, L. J. (2012). *J. Appl. Cryst.* **45**, 849–854.
Hathwar, V. R., Sist, M., Jørgensen, M. R. V., Mamakhel, A. H., Wang, X., Hoffmann, C. M., Sugimoto, K., Overgaard, J. & Iversen, B. B. (2015). *IUCrJ*, **2**, 563–574.
Hirshfeld, H. L. (1977). *Theor. Chim. Acta*, **44**, 129–138.
Hjouji, M. Y., Djedid, M., Elmsellem, H., Kandri Rodi, Y., Ouzidan, Y., Ouazzani Chahdi, F., Sebbar, N. K., Essassi, E. M., Abdel-Rahman, I. & Hammouti, B. (2016). *J. Mater. Environ. Sci.* **7**, 1425–1435.
Kaim, W. & Kohlmann, S. (1987). *Inorg. Chem.* **26**, 68–77.
Khadiri, A., Saddik, R., Bekkouche, K., Aouniti, A., Hammouti, B., Benchat, N., Bouachrine, M. & Solmaz, R. (2016). *J. Taiwan Inst. Chem. Eng.* **58**, 552–564.

Kore, A. R., Yang, B. & Srinivasan, B. (2015). *Tetrahedron Lett.* **56**, 808–811.
Marino, N., Bruno, R., Bentama, A., Pascual-Álvarez, A., Lloret, F., Julve, M. & De Munno, G. (2019). *CrystEngComm*, **21**, 917–924.
Mastropietro, T. F., Marino, N., Armentano, D., De Munno, G., Yuste, C., Lloret, F. & Julve, M. (2013). *Cryst. Growth Des.* **13**, 270–281.
McKinnon, J. J., Jayatilaka, D. & Spackman, M. A. (2007). *Chem. Commun.* 3814–3816.
Parsons, S., Flack, H. D. & Wagner, T. (2013). *Acta Cryst.* B**69**, 249–259.
Rigaku OD (2015). *CrysAlis PRO*. Rigaku Oxford Diffraction, Yarnton, England.
Sheldrick, G. M. (2008). *Acta Cryst.* A**64**, 112–122.
Sheldrick, G. M. (2015). *Acta Cryst*. C**71**, 3–8.
Showrilu, K., Rajarajan, K., Martin Britto Dhas, S. A. & Athimoolam, S. (2017). *IUCrData*, **2**, x171142.
Sikine, M., Elmsellem, H., Kandri Rodi, Y., Steli, H., Aouniti, A., Hammouti, B., Ouzidan, Y., Ouazzani Chahdi, F., Bourass, M. & Essassi, E. M. (2016). *J. Mater. Environ. Sci.* **7**, 4620–4632.
Spackman, M. A. & Jayatilaka, D. (2009). *CrystEngComm*, **11**, 19–32.
Spek, A. L. (2015). *Acta Cryst.* C**71**, 9–18.
Tsukada, N., Sato, T., Mori, H., Sugawara, S., Kabuto, C., Miyano, S. & Inoue, Y. (2001). *J. Organomet. Chem.* **627**, 121–126.
Turner, M. J., McKinnon, J. J., Wolff, S. K., Grimwood, D. J., Spackman, P. R., Jayatilaka, D. & Spackman, M. A. (2017). *CrystalExplorer17*. The University of Western Australia.
Venkatesan, P., Thamotharan, S., Ilangovan, A., Liang, H. & Sundius, T. (2016). *Spectrochim. Acta Part A*, **153**, 625–636.

supporting information

Acta Cryst. (2019). E**75**, 1169-1174 [https://doi.org/10.1107/S2056989019009848]

Crystal structure, Hirshfeld surface analysis and corrosion inhibition study of 3,6-bis(pyridin-2-yl)-4-{[(3a*S*,5*S*,5a*R*,8a*R*,8b*S*)-2,2,7,7-tetramethyltetrahydro-5*H*-bis[1,3]dioxolo[4,5-*b*:4′,5′-*d*]pyran-5-yl)methoxy]methyl}pyridazine monohydrate

Mouad Filali, Hicham Elmsellem, Tuncer Hökelek, Abdelkrim El-Ghayoury, Oleh Stetsiuk, El Mestafa El Hadrami and Abdessalam Ben-Tama

Computing details

Data collection: *CrysAlis PRO* (Rigaku OD, 2015); cell refinement: *CrysAlis PRO* (Rigaku OD, 2015); data reduction: *CrysAlis PRO* (Rigaku OD, 2015); program(s) used to solve structure: *SHELXS97* (Sheldrick, 2008); program(s) used to refine structure: *SHELXL2018* (Sheldrick, 2015); molecular graphics: *ORTEP-3* for Windows (Farrugia, 2012) and *PLATON* (Spek, 2015); software used to prepare material for publication: *WinGX* (Farrugia, 2012) and *PLATON* (Spek, 2015).

3,6-Bis(pyridin-2-yl)-4-{[(3a*S*,5*S*,5a*R*,8a*R*,8b*S*)-2,2,7,7-tetramethyltetrahydro-5*H*-bis[1,3]dioxolo[4,5-*b*:4′,5′-*d*]pyran-5-yl)methoxy]methyl}pyridazine monohydrate

Crystal data

$C_{27}H_{30}N_4O_6 \cdot H_2O$	D_x = 1.354 Mg m^{-3}
M_r = 524.56	Cu $K\alpha$ radiation, λ = 1.54184 Å
Orthorhombic, $P2_12_12_1$	Cell parameters from 2843 reflections
a = 8.8417 (3) Å	θ = 3.3–72.3°
b = 11.3252 (3) Å	μ = 0.82 mm^{-1}
c = 25.7003 (8) Å	T = 150 K
V = 2573.47 (14) Å^3	Plate, colourless
Z = 4	0.47 × 0.15 × 0.10 mm
F(000) = 1112	

Data collection

Rigaku Oxford Diffraction SuperNova, single source at offset, AtlasS2 diffractometer	T_{min} = 0.656, T_{max} = 1.000
	6128 measured reflections
	4277 independent reflections
Radiation source: SuperNova(Cu) micro-focus sealed X-ray Source	3853 reflections with $I > 2\sigma(I)$
	R_{int} = 0.037
Detector resolution: 5.1990 pixels mm^{-1}	θ_{max} = 72.4°, θ_{min} = 3.4°
ω scans	h = −9→10
Absorption correction: multi-scan (CrysAlis PRO (Rigaku OD, 2015)	k = −13→5
	l = −31→29

Refinement

Refinement on F^2
Least-squares matrix: full
$R[F^2 > 2\sigma(F^2)] = 0.048$
$wR(F^2) = 0.121$
$S = 1.10$
4277 reflections
353 parameters
2 restraints
Hydrogen site location: mixed
H atoms treated by a mixture of independent and constrained refinement
$w = 1/[\sigma^2(F_o^2) + (0.0538P)^2 + 0.4885P]$ where $P = (F_o^2 + 2F_c^2)/3$
$(\Delta/\sigma)_{max} < 0.001$
$\Delta\rho_{max} = 0.27$ e Å^{-3}
$\Delta\rho_{min} = -0.36$ e Å^{-3}
Absolute structure: Flack x determined using 1226 quotients $[(I^+)-(I^-)]/[(I^+)+(I^-)]$ (Parsons et al., 2013)
Absolute structure parameter: −0.01 (16)

Special details

Geometry. All esds (except the esd in the dihedral angle between two l.s. planes) are estimated using the full covariance matrix. The cell esds are taken into account individually in the estimation of esds in distances, angles and torsion angles; correlations between esds in cell parameters are only used when they are defined by crystal symmetry. An approximate (isotropic) treatment of cell esds is used for estimating esds involving l.s. planes.

Fractional atomic coordinates and isotropic or equivalent isotropic displacement parameters (Å^2)

	x	y	z	U_{iso}*/U_{eq}
O1	0.3541 (3)	0.1622 (2)	0.41689 (9)	0.0282 (5)
O2	0.3948 (3)	0.34989 (19)	0.45130 (10)	0.0314 (5)
O3	0.6462 (3)	0.30998 (18)	0.44345 (9)	0.0275 (5)
O4	0.5889 (3)	0.00085 (19)	0.47272 (8)	0.0298 (5)
O5	0.5504 (4)	−0.04337 (19)	0.38768 (10)	0.0397 (7)
O6	0.2874 (3)	0.20336 (19)	0.30710 (9)	0.0341 (6)
N1	0.0414 (3)	0.4001 (2)	0.16743 (11)	0.0279 (6)
N2	0.0957 (3)	0.5016 (2)	0.18697 (10)	0.0280 (6)
N3	0.3589 (4)	0.6013 (3)	0.28330 (11)	0.0324 (6)
N4	0.0746 (4)	0.0864 (2)	0.17094 (12)	0.0358 (7)
C1	0.4587 (4)	0.1547 (3)	0.37413 (12)	0.0258 (7)
H1	0.495093	0.234348	0.366098	0.031*
C2	0.4106 (4)	0.2260 (3)	0.45945 (13)	0.0277 (7)
H2	0.355033	0.203400	0.490891	0.033*
C3	0.5408 (4)	0.4049 (3)	0.44788 (14)	0.0310 (7)
C4	0.5790 (4)	0.2100 (3)	0.46886 (12)	0.0246 (6)
H4	0.600843	0.212023	0.506234	0.030*
C5	0.6463 (4)	0.0999 (3)	0.44448 (12)	0.0254 (6)
H5	0.756973	0.102135	0.446060	0.031*
C6	0.5926 (4)	0.0790 (3)	0.38885 (12)	0.0272 (7)
H6	0.676097	0.092996	0.364527	0.033*
C7	0.5754 (4)	−0.0947 (3)	0.43729 (13)	0.0310 (7)
C8	0.4413 (5)	−0.1669 (4)	0.4525 (2)	0.0550 (12)
H8A	0.453499	−0.194150	0.487614	0.082*
H8B	0.432577	−0.233440	0.429569	0.082*
H8C	0.351559	−0.119463	0.450095	0.082*
C9	0.7193 (5)	−0.1667 (3)	0.43584 (15)	0.0394 (9)
H9A	0.802843	−0.116353	0.427016	0.059*

H9B	0.709878	−0.227881	0.410208	0.059*
H9C	0.736583	−0.201467	0.469376	0.059*
C10	0.5503 (5)	0.4786 (3)	0.39910 (15)	0.0427 (9)
H10A	0.650263	0.510885	0.395892	0.064*
H10B	0.478045	0.541722	0.400967	0.064*
H10C	0.528653	0.430067	0.369395	0.064*
C11	0.5698 (5)	0.4759 (3)	0.49680 (16)	0.0442 (9)
H11A	0.569729	0.424125	0.526380	0.066*
H11B	0.491803	0.534147	0.500856	0.066*
H11C	0.666221	0.514400	0.494189	0.066*
C12	0.3729 (4)	0.1086 (3)	0.32779 (13)	0.0286 (7)
H12A	0.442659	0.078782	0.301797	0.034*
H12B	0.306342	0.044768	0.338237	0.034*
C13	0.2122 (4)	0.1736 (3)	0.26014 (13)	0.0275 (7)
H13A	0.122273	0.127514	0.267550	0.033*
H13B	0.278292	0.127130	0.238042	0.033*
C14	0.1697 (4)	0.2873 (3)	0.23325 (12)	0.0253 (6)
C15	0.0791 (4)	0.2958 (3)	0.18820 (12)	0.0247 (6)
C16	0.1872 (4)	0.4980 (3)	0.22846 (12)	0.0247 (6)
C17	0.2238 (4)	0.3919 (3)	0.25319 (12)	0.0263 (6)
H17	0.284224	0.391984	0.282822	0.032*
C18	0.2537 (4)	0.6114 (3)	0.24658 (12)	0.0265 (7)
C19	0.2107 (4)	0.7197 (3)	0.22546 (14)	0.0315 (7)
H19	0.135761	0.723846	0.200145	0.038*
C20	0.2823 (5)	0.8210 (3)	0.24304 (15)	0.0380 (8)
H20	0.256630	0.894499	0.229490	0.046*
C21	0.3920 (4)	0.8114 (3)	0.28088 (15)	0.0376 (9)
H21	0.441630	0.877961	0.293426	0.045*
C22	0.4265 (5)	0.7001 (3)	0.29975 (14)	0.0349 (8)
H22	0.500690	0.693707	0.325247	0.042*
C23	0.0175 (4)	0.1927 (3)	0.15887 (12)	0.0253 (7)
C24	−0.0897 (4)	0.2085 (3)	0.12003 (13)	0.0325 (7)
H24	−0.126828	0.283313	0.112401	0.039*
C25	−0.1402 (5)	0.1107 (3)	0.09294 (14)	0.0378 (8)
H25	−0.211674	0.119110	0.066653	0.045*
C26	−0.0836 (5)	0.0004 (3)	0.10520 (14)	0.0375 (8)
H26	−0.116014	−0.066836	0.087656	0.045*
C27	0.0224 (5)	−0.0065 (3)	0.14423 (15)	0.0414 (9)
H27	0.060342	−0.080694	0.152640	0.050*
O7	0.0146 (4)	0.1893 (3)	0.38725 (14)	0.0542 (8)
H7A	−0.011 (7)	0.141 (5)	0.3642 (19)	0.081*
H7B	0.111 (3)	0.189 (6)	0.386 (2)	0.081*

Atomic displacement parameters (Å^2)

	U^{11}	U^{22}	U^{33}	U^{12}	U^{13}	U^{23}
O1	0.0250 (11)	0.0272 (10)	0.0325 (11)	−0.0023 (10)	−0.0016 (10)	−0.0023 (9)
O2	0.0294 (12)	0.0210 (10)	0.0438 (13)	0.0057 (9)	−0.0026 (11)	−0.0024 (9)

O3	0.0280 (11)	0.0181 (10)	0.0364 (12)	0.0007 (9)	0.0010 (10)	0.0006 (9)
O4	0.0419 (14)	0.0190 (9)	0.0286 (11)	−0.0011 (10)	−0.0005 (11)	0.0020 (8)
O5	0.0627 (18)	0.0179 (10)	0.0385 (13)	0.0041 (11)	−0.0184 (14)	−0.0038 (9)
O6	0.0499 (15)	0.0190 (9)	0.0333 (12)	0.0033 (11)	−0.0182 (12)	−0.0023 (9)
N1	0.0324 (15)	0.0203 (12)	0.0310 (13)	−0.0004 (11)	−0.0037 (13)	−0.0002 (10)
N2	0.0339 (16)	0.0192 (11)	0.0310 (13)	0.0005 (11)	0.0006 (13)	−0.0010 (10)
N3	0.0367 (16)	0.0252 (13)	0.0352 (14)	−0.0026 (12)	−0.0011 (13)	−0.0045 (11)
N4	0.0485 (18)	0.0212 (12)	0.0377 (15)	0.0021 (13)	−0.0154 (15)	−0.0018 (11)
C1	0.0331 (17)	0.0180 (12)	0.0265 (15)	−0.0010 (13)	−0.0025 (14)	0.0020 (11)
C2	0.0333 (17)	0.0201 (13)	0.0298 (15)	0.0016 (13)	0.0036 (15)	−0.0006 (12)
C3	0.0324 (18)	0.0192 (13)	0.0415 (18)	0.0039 (14)	−0.0005 (16)	−0.0011 (13)
C4	0.0299 (16)	0.0179 (12)	0.0260 (14)	−0.0003 (13)	−0.0018 (14)	−0.0005 (11)
C5	0.0295 (16)	0.0188 (13)	0.0280 (15)	0.0026 (13)	0.0008 (14)	0.0019 (12)
C6	0.0333 (18)	0.0209 (13)	0.0274 (15)	0.0010 (13)	−0.0001 (14)	−0.0005 (12)
C7	0.0382 (19)	0.0194 (13)	0.0354 (17)	0.0006 (14)	−0.0015 (16)	−0.0004 (12)
C8	0.047 (2)	0.0365 (19)	0.081 (3)	−0.012 (2)	0.017 (2)	−0.020 (2)
C9	0.044 (2)	0.0321 (17)	0.042 (2)	0.0111 (17)	−0.0034 (18)	0.0023 (15)
C10	0.051 (2)	0.0257 (16)	0.051 (2)	0.0042 (16)	0.002 (2)	0.0079 (15)
C11	0.051 (2)	0.0317 (17)	0.050 (2)	0.0028 (18)	−0.007 (2)	−0.0124 (16)
C12	0.0360 (18)	0.0191 (12)	0.0307 (15)	0.0030 (13)	−0.0085 (15)	0.0024 (12)
C13	0.0331 (17)	0.0174 (13)	0.0319 (16)	−0.0019 (13)	−0.0062 (14)	0.0005 (12)
C14	0.0270 (16)	0.0224 (14)	0.0265 (15)	0.0009 (13)	−0.0004 (13)	0.0014 (12)
C15	0.0269 (16)	0.0194 (13)	0.0277 (14)	0.0000 (13)	−0.0005 (14)	−0.0013 (12)
C16	0.0265 (16)	0.0212 (13)	0.0265 (14)	−0.0003 (12)	0.0026 (13)	−0.0020 (11)
C17	0.0297 (16)	0.0220 (13)	0.0272 (15)	0.0006 (13)	−0.0020 (14)	−0.0011 (12)
C18	0.0285 (16)	0.0217 (14)	0.0293 (15)	−0.0001 (12)	0.0037 (14)	−0.0029 (12)
C19	0.0348 (18)	0.0208 (14)	0.0389 (17)	−0.0005 (15)	−0.0010 (16)	−0.0021 (13)
C20	0.043 (2)	0.0209 (15)	0.050 (2)	−0.0014 (15)	0.0039 (18)	−0.0021 (14)
C21	0.039 (2)	0.0247 (15)	0.049 (2)	−0.0039 (14)	0.0037 (18)	−0.0108 (14)
C22	0.0395 (19)	0.0276 (15)	0.0375 (17)	−0.0033 (16)	−0.0026 (16)	−0.0073 (14)
C23	0.0262 (16)	0.0238 (14)	0.0259 (14)	−0.0037 (12)	0.0008 (13)	0.0003 (12)
C24	0.0327 (18)	0.0295 (15)	0.0353 (16)	0.0029 (15)	−0.0075 (15)	−0.0002 (14)
C25	0.0383 (19)	0.0395 (18)	0.0358 (18)	−0.0010 (17)	−0.0148 (17)	−0.0026 (15)
C26	0.049 (2)	0.0271 (15)	0.0366 (17)	−0.0079 (17)	−0.0059 (18)	−0.0080 (14)
C27	0.058 (3)	0.0234 (15)	0.0428 (19)	0.0013 (16)	−0.015 (2)	−0.0027 (15)
O7	0.0524 (18)	0.0479 (16)	0.0623 (19)	0.0030 (15)	−0.0015 (16)	−0.0140 (14)

Geometric parameters (Å, º)

O1—C2	1.403 (4)	C9—H9B	0.9600
O1—C1	1.439 (4)	C9—H9C	0.9600
O2—C2	1.425 (4)	C10—H10A	0.9600
O2—C3	1.437 (4)	C10—H10B	0.9600
O3—C3	1.428 (4)	C10—H10C	0.9600
O3—C4	1.436 (4)	C11—H11A	0.9600
O4—C7	1.419 (4)	C11—H11B	0.9600
O4—C5	1.430 (4)	C11—H11C	0.9600
O5—C7	1.418 (4)	C12—H12A	0.9700

O5—C6	1.436 (4)	C12—H12B	0.9700
O6—C12	1.416 (4)	C13—C14	1.509 (4)
O6—C13	1.418 (4)	C13—H13A	0.9700
N1—C15	1.339 (4)	C13—H13B	0.9700
N1—N2	1.343 (4)	C14—C17	1.377 (4)
N2—C16	1.339 (4)	C14—C15	1.411 (4)
N3—C18	1.330 (5)	C15—C23	1.493 (4)
N3—C22	1.337 (5)	C16—C17	1.397 (4)
N4—C27	1.339 (5)	C16—C18	1.488 (4)
N4—C23	1.341 (4)	C17—H17	0.9300
C1—C12	1.506 (5)	C18—C19	1.394 (5)
C1—C6	1.510 (5)	C19—C20	1.386 (5)
C1—H1	0.9800	C19—H19	0.9300
C2—C4	1.519 (5)	C20—C21	1.378 (6)
C2—H2	0.9800	C20—H20	0.9300
C3—C10	1.508 (5)	C21—C22	1.385 (5)
C3—C11	1.514 (5)	C21—H21	0.9300
C4—C5	1.517 (4)	C22—H22	0.9300
C4—H4	0.9800	C23—C24	1.388 (5)
C5—C6	1.525 (4)	C24—C25	1.382 (5)
C5—H5	0.9800	C24—H24	0.9300
C6—H6	0.9800	C25—C26	1.383 (5)
C7—C8	1.492 (6)	C25—H25	0.9300
C7—C9	1.512 (5)	C26—C27	1.375 (6)
C8—H8A	0.9600	C26—H26	0.9300
C8—H8B	0.9600	C27—H27	0.9300
C8—H8C	0.9600	O7—H7A	0.84 (2)
C9—H9A	0.9600	O7—H7B	0.86 (2)

O1···O3	3.153 (2)	C2···C4^{ii}	3.538 (4)
O1···O4	3.115 (3)	C2···H4^{ii}	2.96
O1···O5	2.999 (3)	C3···H1	2.88
O1···O6	2.920 (3)	C4···H11A	2.84
O3···O1	3.153 (2)	C4···H2^{iii}	2.83
O3···C1	3.002 (3)	C4···H1	2.76
O7···O1	3.112 (3)	C5···H9A	2.85
O7···O6	3.176 (3)	C10···H1	2.93
O7···N2^{i}	3.020 (3)	H1···H10C	2.24
O2···H1	2.70	H2···H4^{ii}	2.44
O2···H4^{ii}	2.90	H4···H11A	2.47
O3···H1	2.54	H5···H9A	2.56
O3···H2^{iii}	2.51	H7A···H19^{i}	2.20
O5···H12B	2.70	H7A···N1^{i}	2.84 (3)
O5···H12A	2.77	H7A···N2^{i}	2.19 (4)
O6···H17	2.23	H7B···O1	2.30 (2)
O7···H19^{i}	2.64	H7B···O6	2.56 (4)
N4···C13	2.776 (3)	H8A···H9C	2.55
N1···H24	2.44	H8B···H9B	2.50

N2···H19	2.56	H8C···H11C[ii]	2.48
N3···H17	2.46	H10A···H11C	2.53
N4···H13A	2.56	H10B···H11B	2.57
N4···H13B	2.54	H12A···H13B	2.26
C1···C3	3.485 (3)		

C2—O1—C1	113.4 (2)	H10A—C10—H10B	109.5
C2—O2—C3	110.4 (2)	C3—C10—H10C	109.5
C3—O3—C4	106.7 (2)	H10A—C10—H10C	109.5
C7—O4—C5	107.6 (2)	H10B—C10—H10C	109.5
C7—O5—C6	109.6 (2)	C3—C11—H11A	109.5
C12—O6—C13	112.9 (2)	C3—C11—H11B	109.5
C15—N1—N2	121.1 (3)	H11A—C11—H11B	109.5
C16—N2—N1	119.2 (3)	C3—C11—H11C	109.5
C18—N3—C22	117.7 (3)	H11A—C11—H11C	109.5
C27—N4—C23	117.2 (3)	H11B—C11—H11C	109.5
O1—C1—C12	107.5 (3)	O6—C12—C1	107.7 (2)
O1—C1—C6	110.3 (2)	O6—C12—H12A	110.2
C12—C1—C6	113.4 (3)	C1—C12—H12A	110.2
O1—C1—H1	108.5	O6—C12—H12B	110.2
C12—C1—H1	108.5	C1—C12—H12B	110.2
C6—C1—H1	108.5	H12A—C12—H12B	108.5
O1—C2—O2	111.0 (3)	O6—C13—C14	107.7 (2)
O1—C2—C4	114.3 (3)	O6—C13—H13A	110.2
O2—C2—C4	103.7 (3)	C14—C13—H13A	110.2
O1—C2—H2	109.2	O6—C13—H13B	110.2
O2—C2—H2	109.2	C14—C13—H13B	110.2
C4—C2—H2	109.2	H13A—C13—H13B	108.5
O3—C3—O2	105.4 (2)	C17—C14—C15	116.4 (3)
O3—C3—C10	108.3 (3)	C17—C14—C13	118.5 (3)
O2—C3—C10	109.9 (3)	C15—C14—C13	125.1 (3)
O3—C3—C11	110.8 (3)	N1—C15—C14	121.9 (3)
O2—C3—C11	109.4 (3)	N1—C15—C23	113.5 (3)
C10—C3—C11	112.8 (3)	C14—C15—C23	124.6 (3)
O3—C4—C5	107.3 (2)	N2—C16—C17	121.9 (3)
O3—C4—C2	103.9 (2)	N2—C16—C18	117.5 (3)
C5—C4—C2	114.6 (3)	C17—C16—C18	120.5 (3)
O3—C4—H4	110.3	C14—C17—C16	119.3 (3)
C5—C4—H4	110.3	C14—C17—H17	120.3
C2—C4—H4	110.3	C16—C17—H17	120.3
O4—C5—C4	107.2 (2)	N3—C18—C19	122.9 (3)
O4—C5—C6	104.1 (2)	N3—C18—C16	115.1 (3)
C4—C5—C6	113.2 (3)	C19—C18—C16	122.0 (3)
O4—C5—H5	110.7	C20—C19—C18	118.5 (3)
C4—C5—H5	110.7	C20—C19—H19	120.8
C6—C5—H5	110.7	C18—C19—H19	120.8
O5—C6—C1	109.8 (3)	C21—C20—C19	119.1 (3)
O5—C6—C5	104.5 (2)	C21—C20—H20	120.5

C1—C6—C5	113.0 (3)	C19—C20—H20	120.5
O5—C6—H6	109.8	C20—C21—C22	118.3 (3)
C1—C6—H6	109.8	C20—C21—H21	120.8
C5—C6—H6	109.8	C22—C21—H21	120.8
O5—C7—O4	106.1 (2)	N3—C22—C21	123.5 (3)
O5—C7—C8	109.6 (4)	N3—C22—H22	118.2
O4—C7—C8	108.4 (3)	C21—C22—H22	118.2
O5—C7—C9	109.3 (3)	N4—C23—C24	122.6 (3)
O4—C7—C9	110.9 (3)	N4—C23—C15	116.6 (3)
C8—C7—C9	112.3 (3)	C24—C23—C15	120.8 (3)
C7—C8—H8A	109.5	C25—C24—C23	118.7 (3)
C7—C8—H8B	109.5	C25—C24—H24	120.7
H8A—C8—H8B	109.5	C23—C24—H24	120.7
C7—C8—H8C	109.5	C24—C25—C26	119.5 (3)
H8A—C8—H8C	109.5	C24—C25—H25	120.3
H8B—C8—H8C	109.5	C26—C25—H25	120.3
C7—C9—H9A	109.5	C27—C26—C25	117.7 (3)
C7—C9—H9B	109.5	C27—C26—H26	121.2
H9A—C9—H9B	109.5	C25—C26—H26	121.2
C7—C9—H9C	109.5	N4—C27—C26	124.4 (3)
H9A—C9—H9C	109.5	N4—C27—H27	117.8
H9B—C9—H9C	109.5	C26—C27—H27	117.8
C3—C10—H10A	109.5	H7A—O7—H7B	104 (6)
C3—C10—H10B	109.5		

C15—N1—N2—C16	−1.1 (5)	O1—C1—C12—O6	77.8 (3)
C2—O1—C1—C12	−167.7 (2)	C6—C1—C12—O6	−160.1 (3)
C2—O1—C1—C6	68.2 (3)	C12—O6—C13—C14	−161.7 (3)
C1—O1—C2—O2	81.1 (3)	O6—C13—C14—C17	8.0 (4)
C1—O1—C2—C4	−35.8 (3)	O6—C13—C14—C15	−172.8 (3)
C3—O2—C2—O1	−115.1 (3)	N2—N1—C15—C14	3.9 (5)
C3—O2—C2—C4	8.1 (3)	N2—N1—C15—C23	−175.6 (3)
C4—O3—C3—O2	−27.7 (3)	C17—C14—C15—N1	−3.3 (5)
C4—O3—C3—C10	−145.2 (3)	C13—C14—C15—N1	177.6 (3)
C4—O3—C3—C11	90.5 (3)	C17—C14—C15—C23	176.1 (3)
C2—O2—C3—O3	11.5 (4)	C13—C14—C15—C23	−3.0 (5)
C2—O2—C3—C10	128.0 (3)	N1—N2—C16—C17	−2.2 (5)
C2—O2—C3—C11	−107.7 (3)	N1—N2—C16—C18	175.7 (3)
C3—O3—C4—C5	154.1 (3)	C15—C14—C17—C16	0.0 (5)
C3—O3—C4—C2	32.4 (3)	C13—C14—C17—C16	179.2 (3)
O1—C2—C4—O3	96.5 (3)	N2—C16—C17—C14	2.7 (5)
O2—C2—C4—O3	−24.4 (3)	C18—C16—C17—C14	−175.2 (3)
O1—C2—C4—C5	−20.2 (4)	C22—N3—C18—C19	−0.8 (5)
O2—C2—C4—C5	−141.2 (3)	C22—N3—C18—C16	177.7 (3)
C7—O4—C5—C4	147.7 (3)	N2—C16—C18—N3	−171.4 (3)
C7—O4—C5—C6	27.5 (3)	C17—C16—C18—N3	6.5 (4)
O3—C4—C5—O4	175.2 (2)	N2—C16—C18—C19	7.1 (5)
C2—C4—C5—O4	−70.0 (3)	C17—C16—C18—C19	−174.9 (3)

O3—C4—C5—C6	−70.5 (3)	N3—C18—C19—C20	0.9 (5)
C2—C4—C5—C6	44.2 (4)	C16—C18—C19—C20	−177.5 (3)
C7—O5—C6—C1	−121.7 (3)	C18—C19—C20—C21	−0.5 (5)
C7—O5—C6—C5	−0.3 (4)	C19—C20—C21—C22	0.1 (5)
O1—C1—C6—O5	76.1 (3)	C18—N3—C22—C21	0.4 (5)
C12—C1—C6—O5	−44.5 (4)	C20—C21—C22—N3	−0.1 (6)
O1—C1—C6—C5	−40.1 (3)	C27—N4—C23—C24	−0.9 (5)
C12—C1—C6—C5	−160.7 (3)	C27—N4—C23—C15	−178.8 (3)
O4—C5—C6—O5	−16.4 (3)	N1—C15—C23—N4	167.1 (3)
C4—C5—C6—O5	−132.5 (3)	C14—C15—C23—N4	−12.4 (5)
O4—C5—C6—C1	102.9 (3)	N1—C15—C23—C24	−10.8 (4)
C4—C5—C6—C1	−13.2 (4)	C14—C15—C23—C24	169.7 (3)
C6—O5—C7—O4	17.2 (4)	N4—C23—C24—C25	0.4 (5)
C6—O5—C7—C8	134.1 (3)	C15—C23—C24—C25	178.2 (3)
C6—O5—C7—C9	−102.4 (3)	C23—C24—C25—C26	0.2 (6)
C5—O4—C7—O5	−28.3 (4)	C24—C25—C26—C27	−0.3 (6)
C5—O4—C7—C8	−146.0 (3)	C23—N4—C27—C26	0.8 (6)
C5—O4—C7—C9	90.3 (3)	C25—C26—C27—N4	−0.3 (7)
C13—O6—C12—C1	174.4 (3)		

Symmetry codes: (i) $-x$, $y-1/2$, $-z+1/2$; (ii) $x-1/2$, $-y+1/2$, $-z+1$; (iii) $x+1/2$, $-y+1/2$, $-z+1$.

Hydrogen-bond geometry (Å, º)

Cg is the centroid of the N3/C18–C22 ring.

D—H···*A*	*D*—H	H···*A*	*D*···*A*	*D*—H···*A*
O7—H7*A*···N2^{i}	0.84 (2)	2.18 (3)	3.019 (4)	172 (6)
O7—H7*B*···O1	0.86 (2)	2.30 (3)	3.112 (4)	157 (6)
O7—H7*B*···O6	0.86 (2)	2.57 (5)	3.176 (5)	129 (5)
C2—H2···O3^{ii}	0.98	2.51	3.444 (4)	160
C12—H12*A*···*Cg*^{iv}	0.97	3.07	3.761 (3)	130

Symmetry codes: (i) $-x$, $y-1/2$, $-z+1/2$; (ii) $x-1/2$, $-y+1/2$, $-z+1$; (iv) $-x+1$, $y-1/2$, $-z+1/2$.